Journal of Alloys and Compounds 503 (2010) 514–518

Contents lists available at ScienceDirect

Journal of Alloys and Compounds

journal homepage: www.elsevier.com/locate/jallcom

Room temperature synthesis of ZnO nanoflowers on Si substrate via seed-layer assisted solution route

Qian Li, Haikuo Sun, Ming Luo, Wenjian Weng*, Kui Cheng, Chenlu Song, Piyi Du, Ge Shen, Gaorong Han

Materials Science and Engineering, Zhejiang University, Zheda Road 38#, Hangzhou 310027, PR China

ARTICLE INFO

Article history:
Received 19 January 2010
Received in revised form 5 May 2010
Accepted 8 May 2010
Available online 20 May 2010

Keywords:
Semiconductors
Nanostructured materials
Chemical synthesis
Luminescence

ABSTRACT

ZnO nanoflowers were grown on Si substrate through the adoption of a ZnO seed-layer with unique morphology and subsequent immersing in suitable growth medium. Depending on the ZnO seed-layers, ZnO nanostructures varied from nanosheets to nanoflowers. The ZnO nanoflower is composed of nanosheets with 20–30 nm in thickness. XRD results revealed a hexagonal phase of these nanostructures. The ZnO nanoflowers can exhibit strong UV and relatively weak visible luminescence at room temperature. The water wettability of the ZnO nanoflowers showed good hydrophilic property without UV illumination.

1. Introduction

ZnO nanostructures have been extensively studied because of their unique properties and promising applications in nanodevices and nanosystems [1–7]. The properties of ZnO nanostructures depend sensitively on both size and shape. Manipulation of their sub-structure and morphology has arisen many interests in recent years [8,9]. So far, a variety of Zn nanostructures such as nanowires, nanorods, nanodots, nanotubes, nanosheets, nanobelts, nanoribbons, nanorings, nanoaeroplanes, nanocombs, nanobridges and nanonails have been synthesized via various physical and chemical fabrication techniques [10–15]. These methods include vapor phase transport process, chemical vapor deposition, thermal evaporation process, electrodeposition, hydrothermal, self-assembly, and template-assisted sol–gel process [16–21]. The vapor methods usually involve sophisticated equipments, complex procedures or rigid experimental conditions. The solution chemical route therefore becomes a promising option for production of nanostructures due to the facile, efficient and less expensive virtues. Two-dimensional (2D) nanostructures, such as nanosheets, nanoplates and their aggregations of ZnO are suggested to be desirable in producing energy storage, data conversion and memory devices owing to their high specific surface area, interesting optical and photocatalytic activities [22,23]. However, studies on 2D ZnO nanostructures are quite less common compared to those on 1D ZnO nanostructures. Moreover, there is even less literature to report the preparation of this kind of nanostructures with prominent optical properties through facile solution chemical method.

In our previous work, we have developed a seed-layer assisted route to prepare 2D ZnO nanosheets on Si substrate at room temperature [24]. This method is based on growing nanostructures on pre-formed seed-layer in a suitable liquid medium. The photoluminescence (PL) spectra of ZnO nanosheets had a high intensity ratio of UV emission to defect emissions. In this paper, this method is extended to prepare novel ZnO nanosheet aggregations, i.e., ZnO nanoflowers, on Si substrate through controlling the morphology of ZnO seed-layer. The formation of the ZnO nanoflowers was characterized and further discussed. The structural, optical and wetting properties of ZnO nanoflowers were also studied.

2. Experimental details

The precursor solution used for ZnO seed-layers was composed of 0.1 M zinc acetate dihydrate ethanol solution with ethanolamine in equimolar of Zn^{2+}. Clean Si wafers were used as substrates. 15 μL precursor solution was spin-coated onto a Si substrate at 6000 rpm for 30 s. Seed-layers with different morphologies were formed after calcination at 500 °C, 750 °C and 1000 °C for 60 min (seeds A–C), respectively. A mixture of 0.1 M $Zn(NO_3)_2$ and 0.4 M NaOH aqueous solutions with pH 13.2 was prepared as the growth medium for growing ZnO nanostructures. Seeds A–C and bare Si substrate without seed-layer were dipped in the above growth medium vertically and soaked for 4 h at room temperature (~25 °C). Then the substrates were washed with deionized water and ethanol thoroughly, and dried in air to obtain the final products (samples A–D).

Phase and crystallinity of ZnO nanostructures were investigated on an X-ray diffractometer (Thermo ARL X'TRA). The morphologies of ZnO nanostructures were examined by field-emission scanning electron microscope (SEM, Hitachi S-4800) and atomic force microscope (AFM, ARTRAY SPI3800N). The structure of nanoflower was observed using a transmission electron microscope (TEM) (JEOL, JEM-2010) equipped with selected area electron diffraction (SEAD). Photoluminescence (PL)

* Corresponding author. Tel.: +86 0571 87953787; fax: +86 0571 87953787.
E-mail address: wengwj@zju.edu.cn (W. Weng).

0925-8388/$ – see front matter © 2010 Elsevier B.V. All rights reserved.
doi:10.1016/j.jallcom.2010.05.043

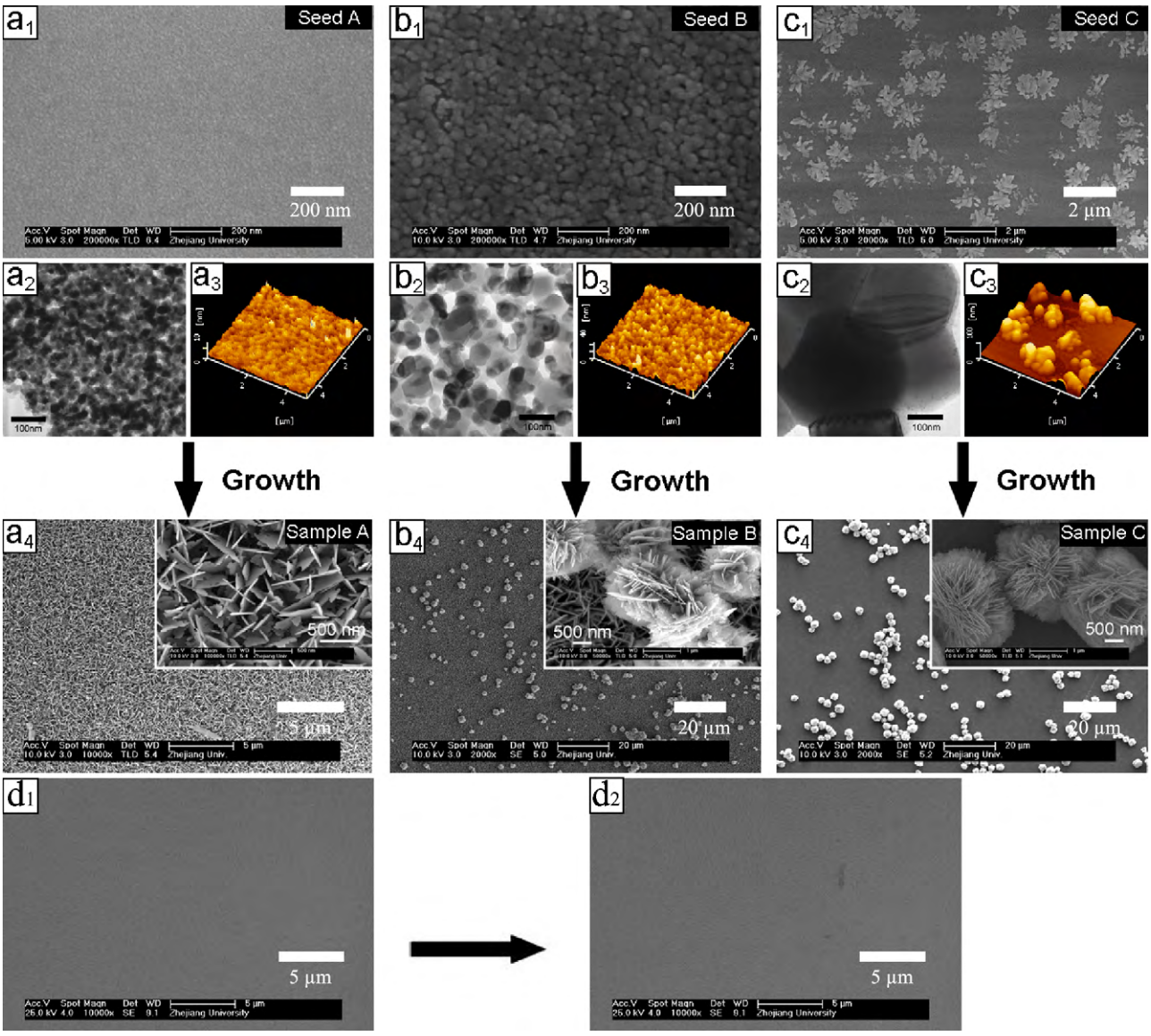

Fig. 1. (a_1–a_3, b_1–b_3, c_1–c_3) SEM, TEM and AFM images of seeds A–C; (a_4, b_4, c_4) SEM images of samples A–C; (d_1,d_2) SEM images of bare Si substrate and sample D.

spectra were performed on a Hitachi F-4500 spectrophotometer using a Xe lamp with a wavelength of 325 nm as the excitation source.

3. Results and discussion

3.1. Formation of ZnO nanoflowers

In our experiment, the control of morphology of ZnO seed-layer plays a key role in the formation of ZnO nanoflowers. Hence, the seed-layers prepared by different procedures were firstly investigated. Fig. 1 shows the SEM (Fig. 1a_1–c_1), TEM (Fig. 1a_2–c_2) and AFM (Fig. 1a_3–c_3) images of ZnO seed-layers calcined at 500 °C (seed A), 750 °C (seed B) and 1000 °C (seed C), respectively. They illustrate that the crystalline grains grew obviously with increase of the calcination temperature. The mean size of crystalline grain of ZnO seed-layer increased from 20 nm to 180 nm when the calcination temperature ascended from 500 °C to1000 °C. Seed A had a continuous coverage of particles with an average size of 20 nm. After calcination at 750 °C, bigger and higher crystal grains formed and a part of the ultrathin films break up into islands with size of 40–80 nm in diameter. In case of seed C which underwent calcination at 1000 °C, the seed-layer film dehisced completely and formed big islands on Si substrate. The grain size exceeds 100 nm from the TEM image shown in Fig. 1c_2. It is assumed that the mobility and surface diffusion of atoms are enhanced under higher temperature, which allows the deposited material to break up and coalesce into larger islands [25]. Abundant grain interfaces exist in the seed-layers, and the fairly high interface energy could be in favor of reducing the system energy of the subsequent ZnO growth in growth medium solution.

Morphologies of ZnO nanostructures (samples A–C) grown on seeds A–C were investigated by SEM (Fig. 1a_4–c_4). They clearly demonstrate that the morphology of ZnO nanostructures varied as a result of the change of seed-layer after the same solution growth. Growing seed A in the solution leads to the formation of ZnO nanosheets with length of 200–600 nm and typical thickness of 20–25 nm (Fig. 1a_4). Each nanosheet has almost the same thickness perpendicular to the substrate, indicating that the nanosheet growth is strictly extended in the 2D plane. When growing seed B in the growth medium, the final product became a compound of ZnO nanosheets and nanoflowers (Fig. 1b_4). The ZnO nanoflowers have the average diameter of about 1–2 μm, and are made up of

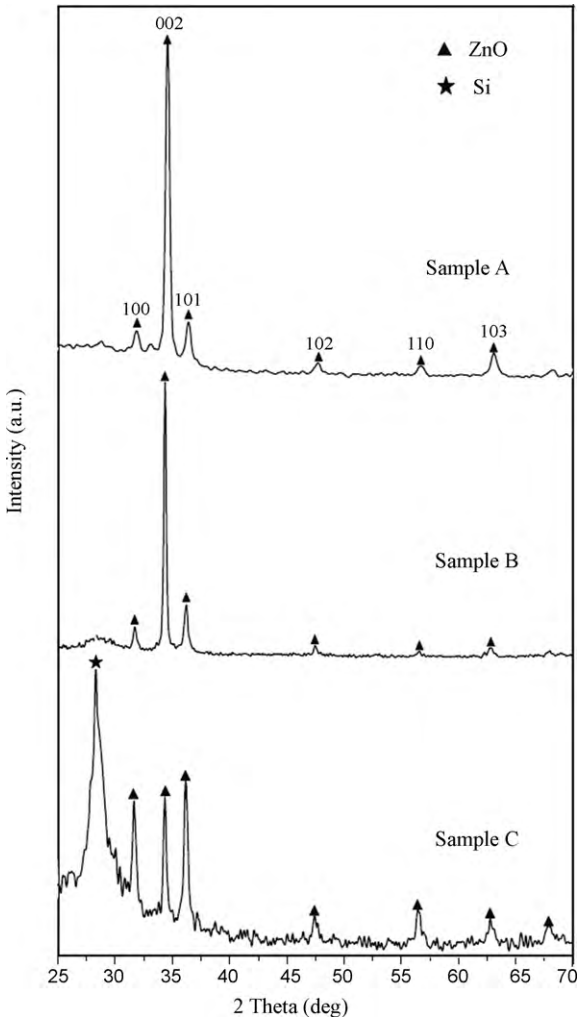

Fig. 2. X-ray diffraction patterns of samples A–C.

spokewise ZnO nanosheets with the mean thickness of 20–25 nm as shown in the magnified image. In the case of seed C, i.e., the 1000 °C calcined island-shaped seed-layer, there is no nanosheet and unique and larger ZnO nanoflowers formed on the Si substrate (Fig. 1c$_4$). From the above data, the grain size of ZnO seeds influences the final morphologies of ZnO nanostructures greatly. The increase of grain size leads to the aggregation of ZnO nanosheets to form the ZnO nanoflowers. SEM images (Fig. 1d$_1$ and d$_2$) show that no nanosheet or nanoflower formed on bare Si substrate without ZnO seed-layer which was soaked in the same growth medium.

3.2. Phase and structure of ZnO nanoflowers

The phase and crystallinity of the obtained ZnO nanostructures grown on different seed-layers were examined using XRD. Fig. 2 shows the XRD patterns of samples A–C. All diffraction peaks can be well indexed to wurtzite structural zinc oxide (hexagonal phase, space group $P6_3mc$). No impurity was detected except for the signals of Si from the substrate, which implies that wurtzite hexagonal ZnO was obtained via this synthetic route. In the cases of samples A and B, the (0 0 2) peak is much stronger than (1 0 0) and (1 0 1) peaks, indicating that most of ZnO crystals grew basically perpendicular to the Si substrate with a preferred growth orientation along the *c*-axis direction. The peak intensity of (0 0 2) plane decreases gradually with morphology transformation from nanosheet to nanoflower. For ZnO nanoflowers, the (1 0 0), (1 0 1) and (0 0 2) peak have the similar intensities, indicating a decreased orientation compared to nanosheets. This may result from the factor that there are less oriented regions in nanoflowers.

Further structural characterization of the ZnO nanoflowers was performed on TEM combined with SAED. Fig. 3a shows the TEM images of ZnO nanoflower and the corresponding magnified image is shown in Fig. 3b. It can be seen that the nanoflower has a spherical shape. Though the nanoflower is mainly composed of nanosheets with 20–30 nm in thickness, there are still some small ZnO sprouts in the body of nanoflower. From the XRD results, it can be deduced that these sprouts are less crystalline-oriented region. Fig. 3c–d shows the high resolution TEM (HRTEM) images of nanosheet in the body of nanoflower. The determined d spacings of 0.28 nm and 0.25 nm correspond to the (0 1 0) and (1 0 1) crystal faces. The SAED pattern is shown in inset of Fig. 3b, which shows that the growth directions are along the [0 1 0] and [1 0 1] crystallographic directions from the inside of the nanoflowers.

3.3. Possible formation mechanism of ZnO nanoflowers

Herein, we propose a possible interpretation to explain the growth mechanism of ZnO nanoflowers. We think that two factors, morphology and crystallite structure of ZnO seed-layer, are dominant. It is considered that the heterogeneous instead of the homogeneous nucleation in solution on the substrate favors the formation of ZnO nanosheets [24]. The degree of supersaturation of the growth medium with pH 13.2 is considered to be low at the initial stage. Therefore, homogeneous nucleation in this solution becomes very difficult [26]. The existence of the ZnO seed-layer can effectively lower the nucleation energy barrier, so it is able to afford heterogeneous nucleation for crystal growth [27]. The 500 °C calcined seed-layer is an ultrathin, continuous and homogeneous film which is composed of many small crystalline grains. These grains act as many active nuclei, resulting into the formation of uniform ZnO nanosheets on Si substrates [24]. In the case of seed B, some of the nuclei aggregated to form bigger grains. During the growth process, the aggregated nanosheets are self-assembled into nanoflowers to decrease the surface energy through reducing exposed area. In this case, both ZnO nanoflowers and nanosheets exist on Si substrate. After calcined at 1000 °C, the seed-layer film broke up completely and formed big islands on the substrate. The high-temperature calcination can induce further aggregation of growth nuclei which contain more active growth seeds compared with seed B. Consequently, seed C can lead to the formation of unique and larger ZnO nanoflowers on substrate.

3.4. Optical properties and wettability of ZnO nanoflowers

Fig. 4 shows the PL spectrum of the ZnO nanoflowers measured at room temperature with an excitation wavelength of 325 nm. Strong UV emission (located at 387 nm) as well as blue emissions (located at about 451 nm and 470 nm) is observed in the PL spectrum. The UV emission generally comes from the direct recombination of free excitons through an exciton–exciton collision process, which is called near band edge emission (NBE) [28]. The appearance of the blue emission results from the impurities and some structural defects (oxygen vacancies and zinc interstitials) in ZnO crystals known as deep level emission [29]. The peak at 451 nm is considered as the electron transition from the shallow donor level of oxygen vacancy and the zinc interstitials to the valence band [30]. The peak around 470 nm is believed to result from the singly ionized oxygen vacancy [31]. Compared with the PL properties of ZnO nanosheets in our previous work [24], the intensity of the blue emission of ZnO nanoflowers increased. We speculate that the stronger blue emission is related to the higher quantity of structural defects in the ZnO nanoflowers.

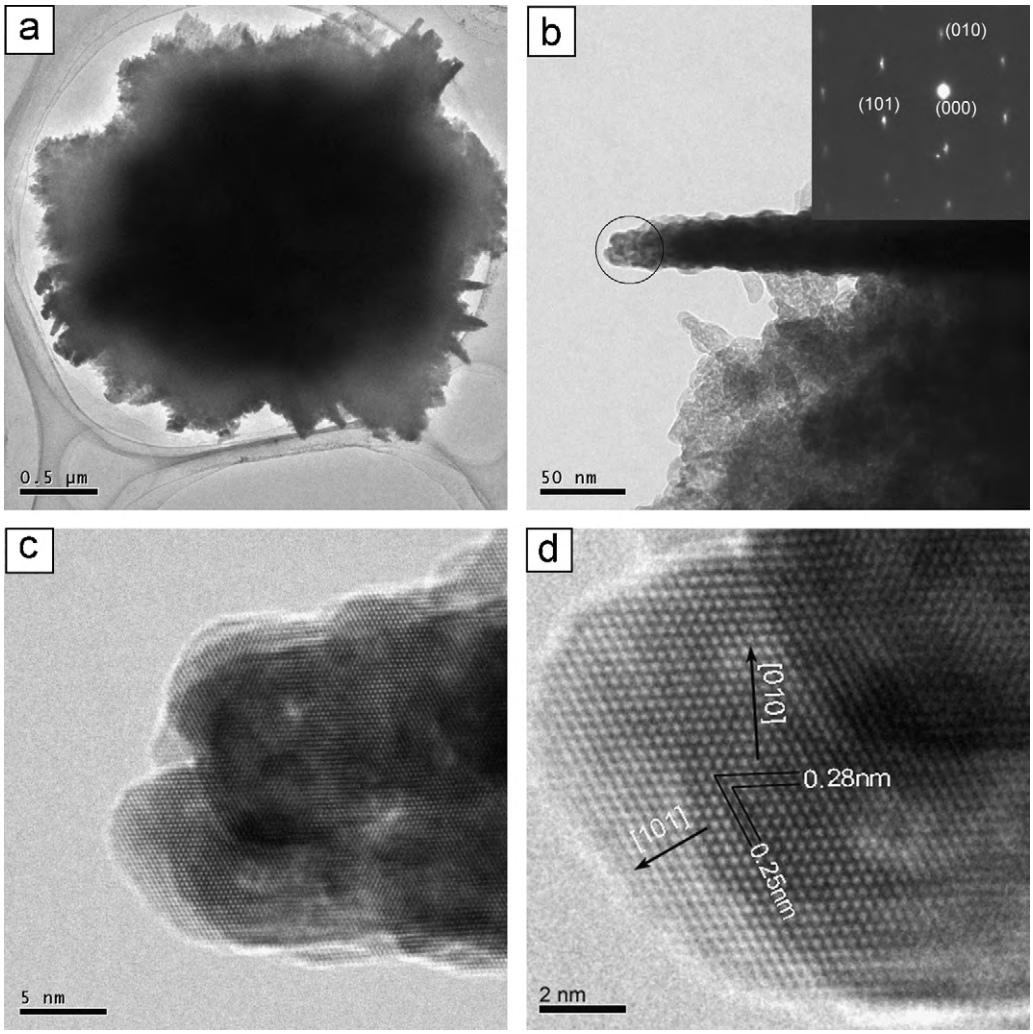

Fig. 3. TEM and HRTEM images of ZnO nanoflowers. Inset of (b) shows the SEAD pattern.

As one of the important properties of a solid surface, wettability is widely studied not only for fundamental research but also for practical applications. The surface wettability is mainly governed by the surface energy and the geometrical structure. Wettability of ZnO nanoflowers on Si substrates was characterized by water contact angle at room temperature, after placing the sample in dark for 3 days. The water contact angle of ZnO nanoflowers film is15.4° (Fig. 5), which demonstrates good hydrophilicity without UV illumination. As reported in literature, the single crystalline

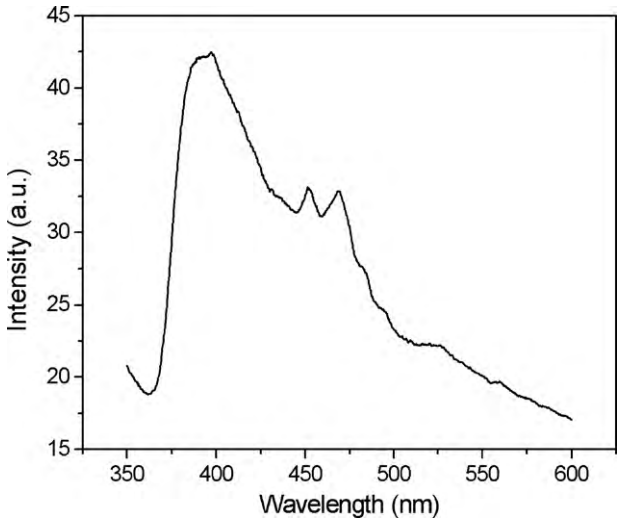

Fig. 4. Room temperature PL spectrum of ZnO nanoflowers.

Fig. 5. Photograph of water droplet shape on a ZnO nanoflower film.

ZnO surface is hydrophilic with the water contact angle to be 31° [32]. Hence, the nanosheet-based ZnO nanoflower structures have an enhanced hydrophilic property. According to Wenzel's model [33], both hydrophobic and hydrophilic properties of a surface can be enhanced by the surface roughness. The increased surface roughness of ZnO nanoflowers can further decrease the water contact angle. Consequently, the surfaces of ZnO nanoflowers become highly hydrophobic.

4. Conclusions

ZnO nanoflowers were prepared on Si substrate via the seed-layer assisted route at room temperature. Control of the morphology of ZnO seed-layer is considered to be the major factor to induce the formation of ZnO nanoflowers. The ZnO nanoflower has the mean diameter of several micrometers and is composed of ZnO nanosheets with 20–30 nm in thickness. The ZnO nanoflower can show strong NBE emission at room temperature. The nanoflower-covered Si substrate showed good hydrophobic property without UV illumination. It is believed that the high-quality ZnO nanoflowers have potential significance in future scientific researches and in applications as optical, optoelectronic and sensing devices.

Acknowledgement

The work was supported by the Nature Science Foundation of China (grant nos. 50572093, 30870627).

References

[1] J.S. L.K., D.B. Janes, M.H. Yoon, A. Facchetti, T.J. Marks, Nano Lett. 5 (2005) 2281.
[2] Q. Ahsanulhaq, J.H. Kim, Y.B. Hahn, Nanotechnology 18 (2007) 485307.
[3] K. Yubuta, T. Sato, A. Nomura, K. Haga, T. Shishido, J. Alloys Compd. 436 (2007) 396.
[4] S. Xu, Z.H. Li, Q. Wang, L.J. Cao, T.M. He, G.T. Zou, J. Alloys Compd. 465 (2008) 56.
[5] C. Klingshirn, Chem. Phys. Chem. 8 (2007) 782.
[6] M. Ristić, S. Musić, M. Ivanda, S. Popović, J. Alloys Compd. 397 (2005) L1.
[7] Y.L. Tao, M. Fu, A.L. Zhao, D.W. He, Y.S. Wang, J. Alloys Compd. 489 (2010) 99.
[8] L.B. Feng, A.H. Liu, M. Liu, Y.Y. Ma, J. Wei, B.Y. Man, J. Alloys Compd. 492 (2010) 427.
[9] Q. Ahsanulhaq, S.H. Kima, Y.B. Hahn, J. Alloys Compd. 484 (2009) 17.
[10] Z.L. Wang, J. Phys.: Condens. Matter 16 (2004) 829.
[11] T. Shishido, K. Yubuta, T. Sato, A. Nomura, J. Ye, K. Haga, J. Alloys Compd. 439 (2007) 227.
[12] Z. Wang, X.F. Qian, J. Yin, Z.K. Zhu, Langmuir 20 (2004) 3441.
[13] C. Cheng, M. Lei, L. Feng, T.L. Wong, K.M. Ho, K.K. Fung, M.T. Loy Michael, D.P. Yu, N. Wang, ACS Nano 3 (2009) 53.
[14] Z. Lockman, Y.P. Fong, T.W. Kian, K. Ibrahim, K.A. Razak, J. Alloys Compd. 493 (2010) 699.
[15] L. Wang, G.C. Liu, L.J. Zou, D.F. Xue, J. Alloys Compd. 493 (2010) 471.
[16] A. Umar, Y.B. Hahn, Nanotechnology 17 (2006) 2174.
[17] H. Tang, J.C. Chang, Y.Y. Shan, D.D.D. Ma, T.Y. Lui, J.A. Zapien, C.S. Lee, S.T. Lee, J. Mater. Sci. 44 (2009) 563.
[18] D.B. Wang, C.X. Song, Z.S. Hu, Cryst. Res. Technol. 43 (2008) 55.
[19] W. Zhao, X.Y. Song, Z.L. Yin, C.H. Fan, G.Z. Chen, S.X. Sun, Mater. Res. Bull. 43 (2008) 3171.
[20] M.S. Mohajerani, A. Lak, A. Simchi, J. Alloys Compd. 485 (2009) 616.
[21] L.R. Singh, R.S. Ningthoujam, S.D. Singh, J. Alloys Compd. 487 (2009) 466.
[22] H.T. Ng, J. Li, M.K. Smith, P. Nguyen, A. Cassell, J. Han, M. Meyyappan, Science 300 (2003) 1249.
[23] J.H. Yang, J.H. Zheng, H.J. Zhai, L.L. Yang, J.H. Lang, M. Gao, J. Alloys Compd. 481 (2009) 628.
[24] H.K. Sun, M. Luo, W.J. Weng, K. Cheng, P.Y. Du, G. Shen, G.R. Han, Nanotechnology 19 (2008) 125603.
[25] I. Szafraniak, C. Harnagea, R. Scholz, S. Bhattacharyya, D. Hesse, M. Alexe, Appl. Phys. Lett. 83 (2003) 2211.
[26] J. Zhao, Z.G. Jin, X.X. Liu, Z.F. Liu, J. Eur. Ceram. Soc. 26 (2006) 3745.
[27] H.K. Sun, M. Luo, W.J. Weng, K. Cheng, P.Y. Du, G. Shen, G.R. Han, Nanotechnology 19 (2008) 395602.
[28] Y.C. Kong, D.P. Yu, B. Zhang, W. Fang, S.Q. Feng, Appl. Phys. Lett. 78 (2001) 407.
[29] D.M. Bagnall, Y.F. Chen, M.Y. Shen, Z. Zhu, T. Goto, T. Yao, J. Cryst. Growth 605 (1998) 184.
[30] D.H. Zhang, Z.Y. Xue, Q.P. Wang, J. Phys. D: Appl. Phys. 35 (2002) 2837.
[31] X. Wang, Q.W. Li, Z.B. Liu, J. Zhang, Z.F. Liu, R.M. Wang, Appl. Phys. Lett. 84 (2004) 4941.
[32] N.S. Pesika, Z. Hu, K.J. Stebe, P.C. Searson, J. Phys. Chem. B 106 (2002) 6985.
[33] R.N. Wenzel, Ind. Eng. Chem. 28 (1936) 988.